

Elsevier Editorial System(tm) for Ceramics International  
Manuscript Draft

Manuscript Number: CERI-D-14-03194

Title: Ultra-high temperature spark plasma sintering of  $\alpha$ -SiC

Article Type: Full Length Article

Keywords: SPS, SiC, PVT, Peltier effect

Corresponding Author: Dr. salvatore Grasso,

Corresponding Author's Institution:

First Author: salvatore Grasso

Order of Authors: salvatore Grasso; Theo Saunders; Harshit Porwal; Michael Reece

Abstract: Ultra High Temperature SPS (UHTSPS) was used to sinter pure  $\alpha$ -SiC at 2450 °C. Such a high temperature and partial vacuum conditions promoted SiC sublimation and condensation reactions. In the presence of an electric field, materials with graded porosity could be produced by using UHTSPS. At high temperature, the condensation of the gaseous species was controlled by the polarity of the applied electric field. Preferential condensation of SiC occurred on the negative electrode (cooler surface) due to the Peltier effect associated with the n-type thermoelectric behaviour of SiC. In absence of an electric field, condensation was driven by gravity and it resulted in dense SiC monoliths.

Suggested Reviewers: Chunfen HU

Director of Powder Technology Laboratory Department of Mechanical Engineering San Diego State University

chfhu@live.cn

expert in Spark Plasma Sintering

Oleg VASYLKIV

NIMS JAPAN

Oleg.VASYLKIV@nims.go.jp

Expert on SiC

Jesus Gonzalez

Institute for Energy and Climate Research (IEK-1) D-52425 Jülich

j.gonzalez@fz-juelich.de

Active in the filed assisted Sintering technology

Milena Salvo

Politecnico di Torino

milena.salvo@polito.it

Many years experience in SiC

Zhipeng Gao

Institute of physics, China Academy of Engineering Physics, Mianyang, 621900, China

z.p.gao@foxmail.com

Experience in thermoelectric properties SiC

Opposed Reviewers:

Dear Editor,

We wish to submit our paper entitled “Ultra-high temperature spark plasma sintering of  $\alpha$ -SiC” to Ceramics International. It is an original work and it describes some directional field effects occurring during the Ultra High Temperature SPS (UHTSPS) of  $\alpha$ -SiC at 2450 °C. Considering the importance of SiC, this work might have several scientific and technological implications.

Our findings can be summarized as follows:

In the presence of an electric field, materials with graded porosity could be produced by using UHTSPS. At high temperature, the condensation of the gaseous species was controlled by the polarity of the applied electric field and it was driven by the Peltier effect associated with the n-type thermoelectric behaviour of SiC. In absence of an electric field, condensation was driven by gravity and it resulted in dense SiC monoliths.

London August, 2014

\*\*\*\*\*

Salvatore Grasso (Ph.D.)

Experienced Researcher

[My papers](#)

+44(0)20 7882 2773

Nanoforce Technology Limited  
Joseph Priestley Building  
Queen Mary, University of London  
Mile End Road London E1 4NS

<http://www.nanoforce.co.uk>

1  
2  
3  
4  
5  
6  
7  
8  
9  
10  
11  
12  
13  
14  
15  
16  
17  
18  
19  
20  
21  
22  
23  
24  
25  
26  
27  
28  
29  
30  
31  
32  
33  
34  
35  
36  
37  
38  
39  
40  
41  
42  
43  
44  
45  
46  
47  
48  
49  
50  
51  
52  
53  
54  
55  
56  
57  
58  
59  
60  
61  
62  
63  
64  
65

## Ultra-high temperature spark plasma sintering of $\alpha$ -SiC

Salvatore Grasso<sup>a,b\*</sup>, Theo Saunders<sup>a,b</sup>, Harshit Porwal<sup>a,b</sup>, Mike Reece<sup>a,b</sup>

<sup>a</sup> School of Engineering and Material Science, Queen Mary University of London, London, E1 4NS, UK

<sup>b</sup>Nanoforce Technology Limited, London, E1 4NS, UK

\* Corresponding author:

Salvatore Grasso (Ph.D.) [s.grasso@nanoforce.co.uk](mailto:s.grasso@nanoforce.co.uk), Nanoforce Technology Limited, Joseph Priestley Building Queen Mary, University of London, Mile End Road London E1 4NS Tel/Fax +44(0)20 7882 2773

### Abstract

Ultra High Temperature SPS (UHTSPS) was used to sinter pure  $\alpha$ -SiC at 2450 °C. Such a high temperature and partial vacuum conditions promoted SiC sublimation and condensation reactions. In the presence of an electric field, materials with graded porosity could be produced by using UHTSPS. At high temperature, the condensation of the gaseous species was controlled by the polarity of the applied electric field. Preferential condensation of SiC occurred on the negative electrode (cooler surface) due to the Peltier effect associated with the n-type thermoelectric behaviour of SiC. In absence of an electric field, condensation was driven by gravity and it resulted in dense SiC monoliths.

## Introduction

Silicon carbide is among the most widely used ceramics for both structural and functional applications. The worldwide yearly consumption of silicon carbide is expected to reach  $2.4 \times 10^6$  tons by 2019 [1]. The main applications for SiC, in terms of volume, are for the steelmaking, refractories and abrasives. A small portion (i.e. a few thousand tonnes) of its production is used for advanced ceramic applications.

Due to its strong covalent bonding, it is difficult to densify SiC without sintering additives. Depending on its application, the typical sintering additives include B, C,  $\text{Al}_2\text{O}_3$  and others rare earth oxides. The powder mixtures are sintered using several techniques with or without applied pressure by solid state or liquid phase sintering [2]. More recently Suzuki et al. [3] successfully densified pure SiC by SPS (1950 °C for 10 minutes under 80 MPa applied pressure) starting from ultrafine grained powder (average particle size 0.2  $\mu\text{m}$ ). They demonstrated the effectiveness of colloidal processing combined with an optimized SPS sintering cycle for achieving fully dense monoliths.

In pressureless conditions, densification of pure SiC is not promoted by increasing the sintering temperature[4]. Recrystallized SiC (RSiC) is produced by firing green bodies in pressureless conditions at temperature up to 2500 °C in vacuum. The result is a porous self-bonded SiC with density comparable to the starting green body ( $2.6 \text{ g/cm}^3$ ). Pressureless sintering results in nearly no shrinkage, thus, large and complex shapes can be manufactured with a certain degree of precision. RSiC has been widely used in metallurgy, aerospace and other industry due to its high temperature strength, outstanding erosion resistance and high oxidation

1  
2  
3  
4 resistance with a continuous use temperature in air up to 1600 °C. The combination of high  
5  
6 thermal conductivity and low coefficient make this material ideal for kiln furniture [1].  
7  
8  
9

10         Semiconductor [5] and nuclear [2, 6] industries require high purity SiC products. To  
11  
12 produce these materials sintering routes are not viable, instead, Chemical Vapor Deposition  
13  
14 (CVD) [7] and Physical Vapour Transport (PVT) techniques are used [8]. These techniques are  
15  
16 also employed to grow large SiC single crystals (i.e. 15 cm diameter discs). The literature on  
17  
18 pressure assisted sintering techniques operating in sublimation temperatures range is quite limited,  
19  
20 this is because such temperatures are barely achievable by conventional apparatuses. In this work  
21  
22 we have developed a novel UHTSPS process able to reach a temperature as high as 2450 °C [9].  
23  
24 At this temperature SPS acted as a PVT growth cell. The UHTSPS gave an insight of the thermo-  
25  
26 electric interactions [10, 11] occurring during the SiC sublimation/condensation reactions. Even  
27  
28 if there is a plenty of literature on both sintering and PVT process of SiC [2], to the authors best  
29  
30 knowledge no paper has been published so far accounting the electric field effects during the  
31  
32 simultaneous events of SiC particles sintering and sublimation/condensation reactions (PVT).  
33  
34 This work aims to fill this gap.  
35  
36  
37  
38  
39  
40  
41  
42

### 43 **Experimental procedure**

44  
45

46         The starting powder of the investigation was UF-10  $\alpha$ -SiC produced by H.C. Starck  
47  
48 (Germany). This powder was produced by the Acheson process, and it mainly consisted of the  $\alpha$ -  
49  
50 polytype. The average particle size measured by laser diffraction analysis (ASTM B 822) was  
51  
52 0.7  $\mu\text{m}$  ( $D_{90\%}=1.8$ ,  $D_{50\%}=0.7$ ,  $D_{10\%}=0.2$ ), the specific surface area was 9.0 - 11  $\text{m}^2/\text{g}$ . The purity  
53  
54 of the starting powder was 98.5 %wt. The main impurities were O (<1.1% wt), Al(<0.03% wt),  
55  
56 Ca (<0.01% wt) and Fe (<0.05% wt).  
57  
58  
59  
60  
61  
62  
63  
64  
65

1  
2  
3  
4 In order to understand the effect of the electric field on the physical vapour transport, two  
5  
6 SPS *configurations* were employed. In both of the *configurations* the temperature was 2450 °C.  
7  
8  
9 All the experiments were carried out using an SPS furnace (HPD 25, FCT Systeme GmbH,  
10  
11 Rauenstein, Germany) in argon partial pressure of 1200 Pa.  
12  
13  
14

15 *Configuration 1* is shown in Figure 1 (a). The as received SiC powder (1 g) was poured in  
16  
17 a hollow graphite die with 20 mm inner diameter. The SiC powder was heated under an applied  
18  
19 uniaxial pressure, resulting in a good electric contact between the sample and the pressing  
20  
21 punches. This allowed the effective application of an electric field across the sintering specimen  
22  
23 as detailed in Ref. [12]. In the UHTSPS configuration, thick graphite felt was employed to  
24  
25 reduce the heat loss by radiation. The UHTSPS experiments were carried out in 2 steps heating  
26  
27 mode, in the first step pressure was kept constant at 16 MPa while heating up to 2000 °C at a rate  
28  
29 of 200 °C/min, in the second step the pressure was linearly increased up to 40 MPa while heating  
30  
31 up to 2450 °C at a rate of 50 °C/min. The dwelling time under 40 MPa was 40 minutes, and the  
32  
33 cooling rate was 100 °C/min. The temperature was measured using a top pyrometer focused  
34  
35 inside a hole in the punch at distance of 4 mm from the sample.  
36  
37  
38  
39  
40  
41  
42

43 *Configuration 2*, is shown in Figure 4 (a). It was designed to minimize the contribution of  
44  
45 the electric current (electric field applied across the compact) on the PVT of SiC. The loosely  
46  
47 packed SiC powder were not in contact with the top punch (i.e. the mould was not completely  
48  
49 filled up) and the powder (1 g) was not pressed between the punches. *Configuration 2* consisted  
50  
51 of a hollow mould with inner and outer diameters of 14 and 20 mm respectively, its height was  
52  
53 20 mm. The mould was pressed between two graphite punches, and the temperature was probed  
54  
55 by the top pyrometer pointing at punch inner wall (point 1 in Figure 4 (a)) and by the surface  
56  
57  
58  
59  
60  
61  
62  
63  
64  
65

1  
2  
3  
4 pyrometer pointing on the outer die wall (point 2 in Figure 4 (a)). The temperature probed at the  
5  
6 die surface was raised up to 2450 °C in 3 minutes and dwelled for 3 minutes.  
7  
8

9  
10 The samples were characterized using an SEM (FEI, Inspect F, Hillsboro, USA).  
11

## 12 **Results and discussion**

13  
14  
15  
16  
17 In order to perform UHTSPS experiments a novel punch die setup was developed. This  
18 configuration aimed to reduce the localized overheating occurring between punch and spacer as  
19 described by Giuntini et al. [13]. The modified SPS set-up consisted of a punch with tronco-  
20 conical shape which is sketched in Figure 1 (a). The UHTSPS set-up avoided overheating and  
21 consequent creep failure of the SPS punch die assembly at temperatures exceeding 2200 °C. The  
22 SPS apparatus applied pulsed unidirectional (rectified) DC current with waveform of 15 ms on  
23 and 5 ms off. The SPS current flows in an upward direction with respect to a gravity, as shown in  
24 Figure 1 (a) the bottom ram of the SPS machine corresponds to the positive electrode.  
25  
26  
27  
28  
29  
30  
31  
32  
33  
34  
35  
36

37 At 2450 °C in partial vacuum conditions volatilization of SiC occurs. In fact, SiC single  
38 crystals are grown using PVT process, which is carried in argon partial pressure of 6700 Pa and  
39 temperature of 2200 °C [14], resulting in deposition rate between 0.2 to 2 mm per hour [15]. In  
40 the PVT process the SiC recrystallization is driven by a thermal gradient created on the surface  
41 of a growth cell (a quasi-closed graphite crucible). Typically the hotter zone (top of the crucible)  
42 is at a temperature higher than 2200 °C while the colder zone (bottom of the crucible) is at a  
43 lower temperature of about 2150 °C with a gradient of 10 °C/cm [5]. It should be noted that the  
44 UHTSPS conditions in terms of both temperature (2450 °C) and vacuum (1200 Pa) promote  
45 greater evaporation rate than the one typically reported for the PVT process. The sublimation not  
46  
47  
48  
49  
50  
51  
52  
53  
54  
55  
56  
57  
58  
59  
60  
61  
62  
63  
64  
65



1  
2  
3  
4 only produces SiC (gas) but also depending on the processing conditions, others molecular  
5  
6 gaseous species (Si, C, SiC<sub>2</sub>, and Si<sub>2</sub>C) [16].  
7  
8  
9

10 Figures 1 show the microstructures observed at the top (b) and the bottom (c) surfaces of  
11 the SiC powder processed by UHTSPS dwelled at 2450 °C for 40 minutes. Comparing the top  
12 surface (a) with the bottom one (b) there is a significant difference in the density. The relative  
13 density estimated by image analysis of the top surface (Figure 1(b)) was 93±5%, while the  
14 bottom surface of the sample was clearly more porous and the relative density was 75%±5%  
15 (Figure 1(c)). As evidenced in Figure 2 (a) the sample had a graded densification along an axial  
16 direction, which indicates a marked directional field effect. Figures 2 shows the cross section of  
17 the samples presented in Figures 1. This confirmed the higher relative density of the top of the  
18 sample 94±5 (Figure 2 (b)) compared to the bottom 74 ± 5% (Figure 2(c)). The arrows in Figure  
19 2 (b,c) point at porosity, which was closed and open at the top and bottom of the sample  
20 respectively. As apparent in Figure 2 (a), the preferential condensation followed the applied  
21 electric field, with sublimation from the bottom with condensation at the top. As modelled by  
22 Maizza et al. [17], no large asymmetric (respect to the sample mid-thickness plane) thermal  
23 gradient is expected to be generated along an axial direction across the sintering sample (see Fig.  
24 24 in their work), so, the preferential densification of the sample should be attributed to other  
25 effects than simple Joule heating.  
26  
27  
28  
29  
30  
31  
32  
33  
34  
35  
36  
37  
38  
39  
40  
41  
42  
43  
44  
45  
46  
47  
48  
49

50 In order to understand in more detail the mechanism related to the preferential density  
51 distribution of the sample, a further UHTSPS run was performed using *configuration 1*. In this  
52 case the sample was heated twice in two separate cycles. Each cycle was performed as detailed  
53 in the experimental condition and the dwell of each cycle was 20 minutes at 2450 °C. During the  
54 second cycle the mould was turned upside down (referred as *turned configuration 1*). This  
55  
56  
57  
58  
59  
60  
61  
62  
63  
64  
65

1  
2  
3  
4 allowed us to investigate whether the preferential density distribution was reproducible with  
5  
6 respect to the applied field. Figures 3 show cross section the samples, obtained using the *turned*  
7  
8 *configuration 1*. The relative density of the region near the top of the sample was  $96\pm 4\%$  (Figure  
9  
10 3 (b)) while the bottom was (d)  $91\pm 5\%$  (Figure 3 (c)). The relative density in the sample mid-  
11  
12 thickness (Figure 3 (c)) was significantly lower and it was  $73 \pm 5 \%$  which is still comparable  
13  
14 with the one shown in Figure 2 (c). By analogy with the results obtained in *configuration 1*,  
15  
16 Figure 3(a) shows open porosity in the central area of the sample, while closed porosity at the  
17  
18 bottom and top surfaces. The results obtained in *configuration 1* and *1 turned* suggest that the  
19  
20 condensation mainly occurred on the top surface of the sample (negative electrode).  
21  
22  
23  
24  
25  
26

27 The polarity of existing SPS hardware could not be inverted (i.e. make the top electrode  
28  
29 positive). This would have been useful to investigate the condensation reaction for different  
30  
31 polarities. In order to overcome this limitation, *Configuration 2* was employed. This  
32  
33 configuration is sketched in Figure 4 (a). The loosely packed SiC powder was heated in a  
34  
35 graphite crucible. There was no pressure applied to the powder since the pressing punches  
36  
37 applied the load through the graphite mould. The powder was heated up to  $2450\text{ }^\circ\text{C}$  (measured at  
38  
39 point 2 in Figure 4 (a)) in 3 die wall minutes and dwelled for 3 minutes. Unlike the experiments  
40  
41 in *configuration 1*, the condensation occurred on the bottom punch as shown in Figure 4 (b).  
42  
43 Residual SiC powder was left in the mould, this suggest that only part of the powder sublimated  
44  
45 and condensed. Figure 4 (c) shows the fracture surface of condensed SiC. The monolith  
46  
47 exhibited a pore free structure as shown in the high magnification inset of Figure 4 (c). As  
48  
49 reported in Ref. [18], SiC condensation is driven by two contributions, the first one is the  
50  
51 temperature gradient between the die wall and the punches, the second one is gravity. During the  
52  
53 SPS experiments the die wall was  $200\text{ }^\circ\text{C}$  hotter than the temperature probed by the top  
54  
55  
56  
57  
58  
59  
60  
61  
62  
63  
64  
65

1  
2  
3  
4 pyrometer. As results, in *configuration 2*, the absence of electric current flowing across the  
5  
6 sample and the symmetric temperature distribution respect to die mid-thickness plane resulted in  
7  
8 a preferential condensation driven by a gravity.  
9

10  
11  
12 Considering the observations in Figures 1-3, it seems that the condensation of SiC  
13  
14 gaseous species might have been driven by an electric field via ionization process where the  
15  
16 gaseous particles acquire a positive charge. However the voltage applied in the SPS is below 10  
17  
18 V and the corresponding electric field across the sample is usually below 5-10 V/cm [12]. Such a  
19  
20 low field strength was probably not sufficient to generate ionization of gaseous species. As  
21  
22 reported by Yasufumi et al. [19], no arcing could be generated in the case of 99% SiC in any  
23  
24 atmosphere even when the voltage was 30 V [20]. For example, the SPS electric field is several  
25  
26 orders of magnitude lower than employed by Yacaman et al. ( $0.2 \cdot 10^4$  V/cm) [21] which affected  
27  
28 the sublimation condensation reaction in the case of ionic crystals.  
29  
30  
31  
32  
33  
34

35 By comparing the results in *configuration 1* and 2, it is possible to conclude that the  
36  
37 electric current directed the condensation on the top punch (negative electrode), while in absence  
38  
39 of an electric current it occurred on the bottom punch (positive electrode). In the presence of an  
40  
41 electric current (*configuration 1*) through the sample, the condensation may have been driven by  
42  
43 the induced thermal gradient generated by Peltier effect resulting from the voltage applied on the  
44  
45 sintering sample. Only a few studies have attempted to quantify the magnitude of the  
46  
47 temperature gradient generated by Peltier effect in the SPS technique [11]. In the case p-type  
48  
49 thermoelectric materials, Becker et al. demonstrated by simulation and experiments, that the  
50  
51 temperature decreased from the negative electrode to the positive one [11]. Here the gradient is  
52  
53 expected to have the opposite sign because of the n-type nature of SiC. It is well known that  
54  
55 pure  $\alpha$ -SiC is a thermoelectric material with n-type behaviour [22]. Pai et al. [23] measured the  
56  
57  
58  
59  
60  
61  
62  
63  
64  
65

1  
2  
3  
4 thermoelectric properties of SiC up to 1000 °C; both the Seebeck coefficient and electrical  
5  
6 conductivity (in absolute value) increase with increasing temperature. As a result of the Peltier  
7  
8 effect, the temperature is expected to be lower on the top electrode (negative) compared to the  
9  
10 bottom one (positive). The latter might explain the preferential condensation on the cooler  
11  
12 electrode as in the case of PVT process. Unfortunately the thermoelectric properties (Seebeck  
13  
14 coefficient, electric and thermal conductivities) of SiC at temperature higher than 1000 °C are  
15  
16 not known, so, the thermal gradient generated in *configuration 1* cannot be quantified. However,  
17  
18 in the case of PVT a small temperature gradient of 1 °C/mm is sufficient to drive the  
19  
20 condensation [18].  
21  
22  
23  
24  
25  
26

## 27 **Conclusions**

28  
29  
30 In the presence of an electric current through the sintering SiC particles, UHTSPS  
31  
32 resulted in preferential condensation driven by the thermal gradient generated by the Peltier  
33  
34 effect associated with the n-type semiconductor behaviour of pure  $\alpha$ -SiC. Comparable results  
35  
36 were obtained even by inverting the orientation of the sample. In the absence of current flowing  
37  
38 through the material, the condensation of SiC was mainly driven by the gravity and resulted in a  
39  
40 pore free material. The newly developed UHTSPS made possible to perform PVT of SiC at high  
41  
42 temperature 2450 °C. The results shows that UHTSPS is an effective tool for manufacturing  
43  
44 high purity SiC either in the form of dense monoliths or materials with graded porosity.  
45  
46  
47  
48  
49  
50

## 51 **Acknowledgement**

52  
53  
54 S.G. was supported by grant No. EP/K008749/1 (Material Systems for Extreme Environments)  
55  
56 from Engineering and Physical Sciences Research Council (EPSRC). T.S. was supported by FP7  
57  
58 2007-2013 (ADMACOM) a European Community's 7th framework Programme.  
59  
60  
61  
62  
63  
64  
65

1  
2  
3  
4  
5  
6  
7  
8 **Figure captions**  
9

10  
11 Figure 1. (a) Schematic of the UHTSPS punch die assembly (*configuration 1*). The polarity of the  
12 punches is also marked in. SEM of the polished sample observed at (a) the top and (b) the  
13 bottom surfaces. The samples were heated processed at 2450 °C for 40 minutes under an applied  
14 pressure of 40 MPa.  
15  
16  
17  
18  
19

20  
21 Figure 2. SEM of sample cross (a) section evidencing graded densification microstructure is  
22 evidenced. Higher magnification images observed at the (b) top surface and (c) the bottom  
23 surfaces confirms the graded density. The sample was processed as in Figure 1.  
24  
25  
26  
27  
28

29  
30 Figure 3. Figure (a) shows a full cross section and it confirms higher density of the top and the  
31 bottom surfaces compared to the sample mid-thickness. Higher magnification images of sample  
32 cross section observed at (b) the top, (c) the middle and (d) the bottom surfaces. The sample was  
33 processed accordingly *configuration 1 inverted*.  
34  
35  
36  
37  
38

39  
40 Figure 4. (a) Schematic of the UHTSPS *configuration 2*. The SiC powder was loosely packed in  
41 a hollow mould and heated to 2450°C and dwelled for 3 minutes. The PVT results in a dense  
42 compact condensed on the bottom punch as highlighted by arrow in Figure (b). The result is a  
43 dense pore free compact as illustrated in Figures (c).  
44  
45  
46  
47  
48  
49  
50  
51  
52  
53  
54  
55  
56  
57  
58  
59  
60  
61  
62  
63  
64  
65

1  
2  
3  
4  
5  
6  
7  
8  
9  
10  
11 **References**  
12  
13

- 14 [1] G.S.M.f.A. Transparency Market Research Report Add "Silicon Carbide (Black SiC, Aerospace, Military,  
15 Electronics, Healthcare, Steel and Energy Applications - Global Industry Analysis, Size, Share, Growth,  
16 Trends and Forecast, 2013 - 2019" to its database.  
17 [2] L.L. Snead, T. Nozawa, Y. Katoh, T.S. Byun, S. Kondo, D.A. Petti, Handbook of SiC properties for fuel  
18 performance modeling, *Journal of Nuclear Materials*, 371 (2007) 329-377.  
19 [3] T.S. Suzuki, T. Uchikoshi, Y. Sakka, Densification of SiC by colloidal processing and SPS without  
20 sintering additives, *Advances in Applied Ceramics*, 113 (2014) 85-88.  
21 [4] Z.Z. Yi, Z.P. Xie, Y. Huang, J.T. Ma, Y.B. Cheng, Study on gelcasting and properties of recrystallized  
22 silicon carbide, *Ceramics International*, 28 (2002) 369-376.  
23 [5] P. Wellmann, P. Desperrier, R. Müller, T. Straubinger, A. Winnacker, F. Baillet, E. Blanquet, J. Marc  
24 Dedulle, M. Pons, SiC single crystal growth by a modified physical vapor transport technique, *Journal of*  
25 *Crystal Growth*, 275 (2005) e555-e560.  
26 [6] S. Grasso, P. Tatarko, S. Rizzo, H. Porwal, C. Hu, Y. Katoh, M. Salvo, M.J. Reece, M. Ferraris, Joining of  
27  $\beta$ -SiC by spark plasma sintering, *Journal of the European Ceramic Society*, 34 (2014) 1681-1686.  
28 [7] C. Hallin, I.G. Ivanov, T. Egilsson, A. Henry, O. Kordina, E. Janzén, The material quality of CVD-grown  
29 SiC using different carbon precursors, *Journal of Crystal Growth*, 183 (1998) 163-174.  
30 [8] G. Augustine, H.M. Hobgood, V. Balakrishna, G. Dunne, R.H. Hopkins, Physical vapor transport growth  
31 and properties of SiC monocrystals of 4H polytype, *Physica Status Solidi (B) Basic Research*, 202 (1997)  
32 137-148.  
33 [9] J. Kriegesmann, Microstructure control during consolidation of fine grained recrystallized silicon  
34 carbide, *Proceedings of the 8th Conference and Exhibition of the European Ceramic Society in Istanbul,*  
35 2003, (2004) 2199-2202.  
36 [10] S. Grasso, Y. Sakka, G. Maizza, Electric current activated/assisted sintering (ECAS): A review of  
37 patents 1906-2008, *Science and Technology of Advanced Materials*, 10 (2009).  
38 [11] A. Becker, S. Angst, A. Schmitz, M. Engenhorst, J. Stoetzel, D. Gautam, H. Wiggers, D.E. Wolf, G.  
39 Schierning, R. Schmechel, The effect of Peltier heat during current activated densification, *Applied*  
40 *Physics Letters*, 101 (2012).  
41 [12] S. Grasso, Y. Sakka, Electric field in SPS: Geometry and pulsed current effects, *Nippon Seramikkusu*  
42 *Kyokai Gakujutsu Ronbunshi/Journal of the Ceramic Society of Japan*, 121 (2013) 524-526.  
43 [13] D. Giuntini, E.A. Olevsky, C. Garcia-Cardona, A.L. Maximenko, M.S. Yurlova, C.D. Haines, D.G. Martin,  
44 D. Kapoor, Localized overheating phenomena and optimization of spark-plasma sintering tooling design,  
45 *Materials*, 6 (2013) 2612-2632.  
46 [14] A. Itoh, H. Matsunami, Single crystal growth of SiC and electronic devices, *Critical Reviews in Solid*  
47 *State and Materials Sciences*, 22 (1997) 111-197.  
48 [15] R.C. Glass, D. Henshall, V.F. Tsvetkov, C.H. Carter Jr, SiC seeded crystal growth, *Physica Status Solidi*  
49 *(B) Basic Research*, 202 (1997) 149-162.  
50 [16] T.S. Sudarshan, S.I. Maximenko, Bulk growth of single crystal silicon carbide, *Microelectronic*  
51 *Engineering*, 83 (2006) 155-159.  
52  
53  
54  
55  
56  
57  
58  
59  
60  
61  
62  
63  
64  
65

- 1  
2  
3  
4 [17] G. Maizza, S. Grasso, Y. Sakka, Moving finite-element mesh model for aiding spark plasma sintering  
5 in current control mode of pure ultrafine WC powder, *Journal of Materials Science*, 44 (2009) 1219-1236.  
6 [18] B. Gao, X.J. Chen, S. Nakano, S. Nishizawa, K. Kakimoto, Analysis of SiC crystal sublimation growth by  
7 fully coupled compressible multi-phase flow simulation, *Journal of Crystal Growth*, 312 (2010) 3349-  
8 3355.  
9 [19] Y. Nariki, Y. Inoue, K. Tanaka, Production of ultra fine SiC powder from SiC bulk by arc-plasma  
10 irradiation under different atmospheres and its application to photocatalysts, *Journal of Materials*  
11 *Science*, 25 (1990) 3101-3104.  
12 [20] K. Tanaka, K. Ishizaki, S. Yumoto, T. Egashira, M. Uda, Production of ultra-fine silicon powder by the  
13 arc plasma method, *Journal of Materials Science*, 22 (1987) 2192-2198.  
14 [21] M.J. Yacamán, Z.A. Munir, T. Ocaña, J.P. Hirth, Sublimation of ionic crystals in the presence of an  
15 electrical field, *Applied Physics Letters*, 34 (1979) 727-728.  
16 [22] H. Kitagawa, N. Kado, Y. Noda, Preparation of N-type silicon carbide-based thermoelectric materials  
17 by Spark Plasma Sintering, *Materials Transactions*, 43 (2002) 3239-3241.  
18 [23] C.-H. Pai, K. Koumoto, H. Yanagida, Effects of sintering additives on the thermoelectric properties of  
19 SiC ceramics, *Nippon Seramikkusu Kyokai Gakujutsu Ronbunshi/Journal of the Ceramic Society of Japan*,  
20 97 (1989) 1170-1175.  
21  
22  
23  
24  
25  
26  
27  
28  
29  
30  
31  
32  
33  
34  
35  
36  
37  
38  
39  
40  
41  
42  
43  
44  
45  
46  
47  
48  
49  
50  
51  
52  
53  
54  
55  
56  
57  
58  
59  
60  
61  
62  
63  
64  
65

Figure 1  
[Click here to download high resolution image](#)

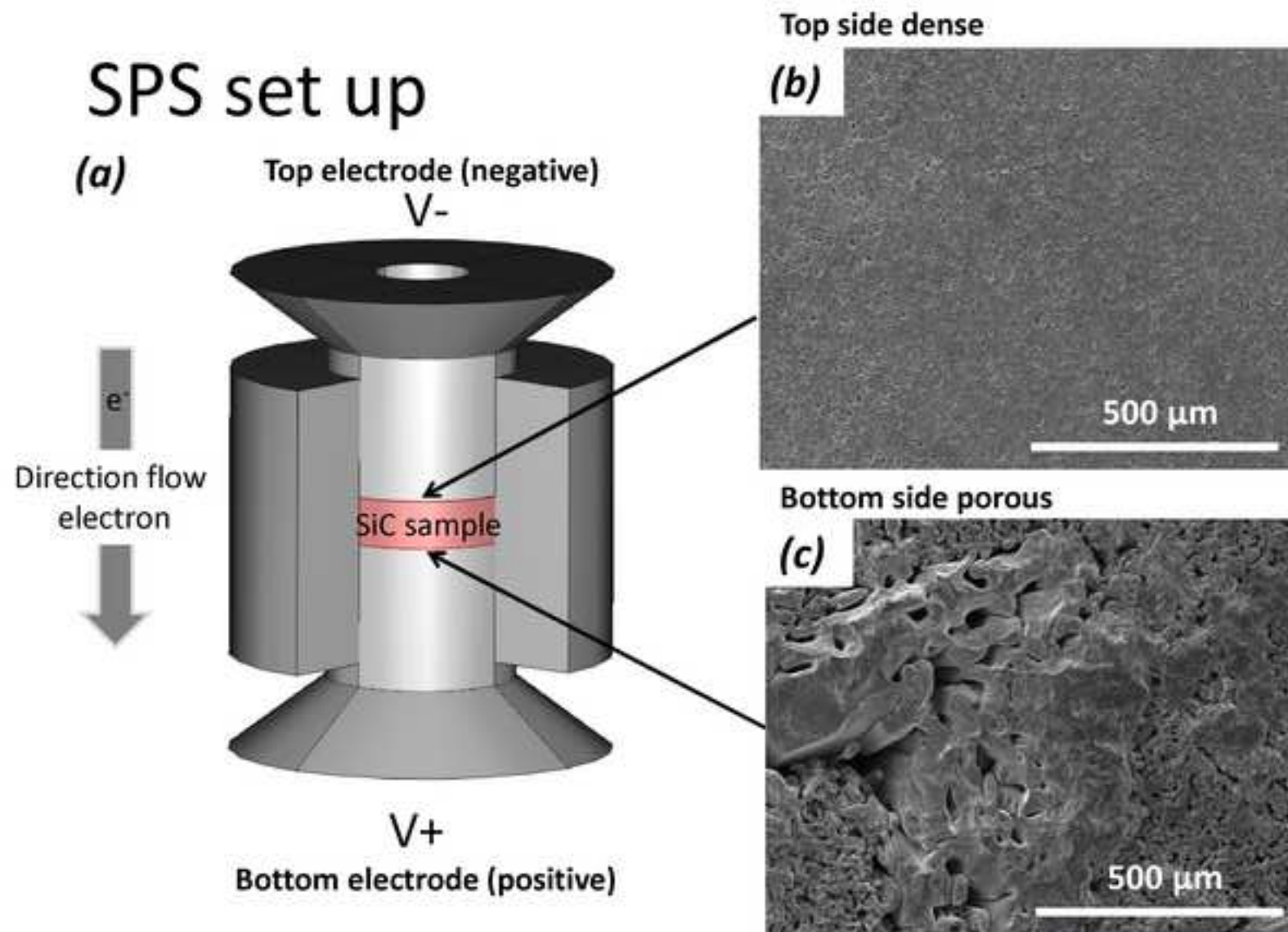




Figure 2  
[Click here to download high resolution image](#)

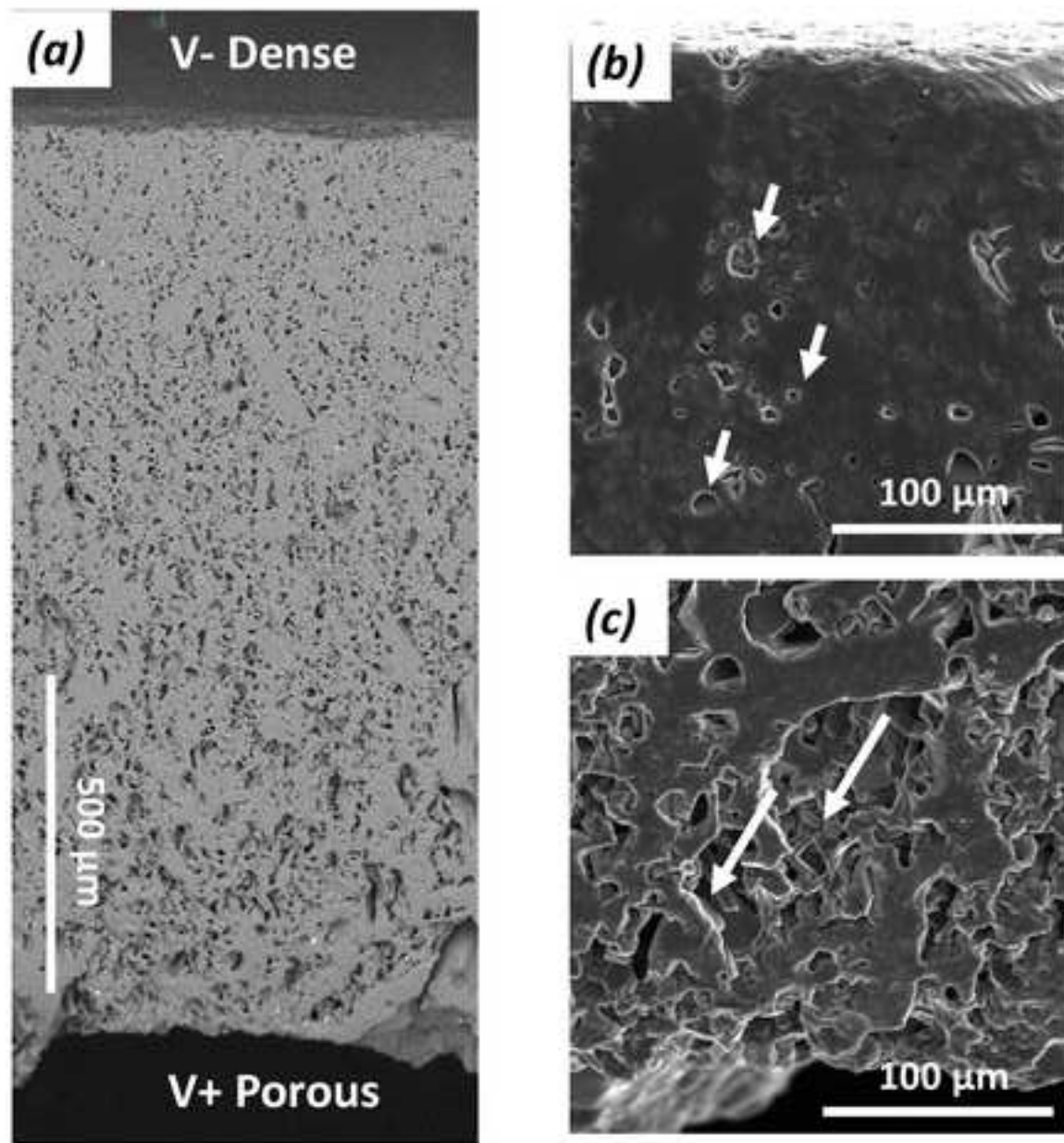


Figure 3  
[Click here to download high resolution image](#)

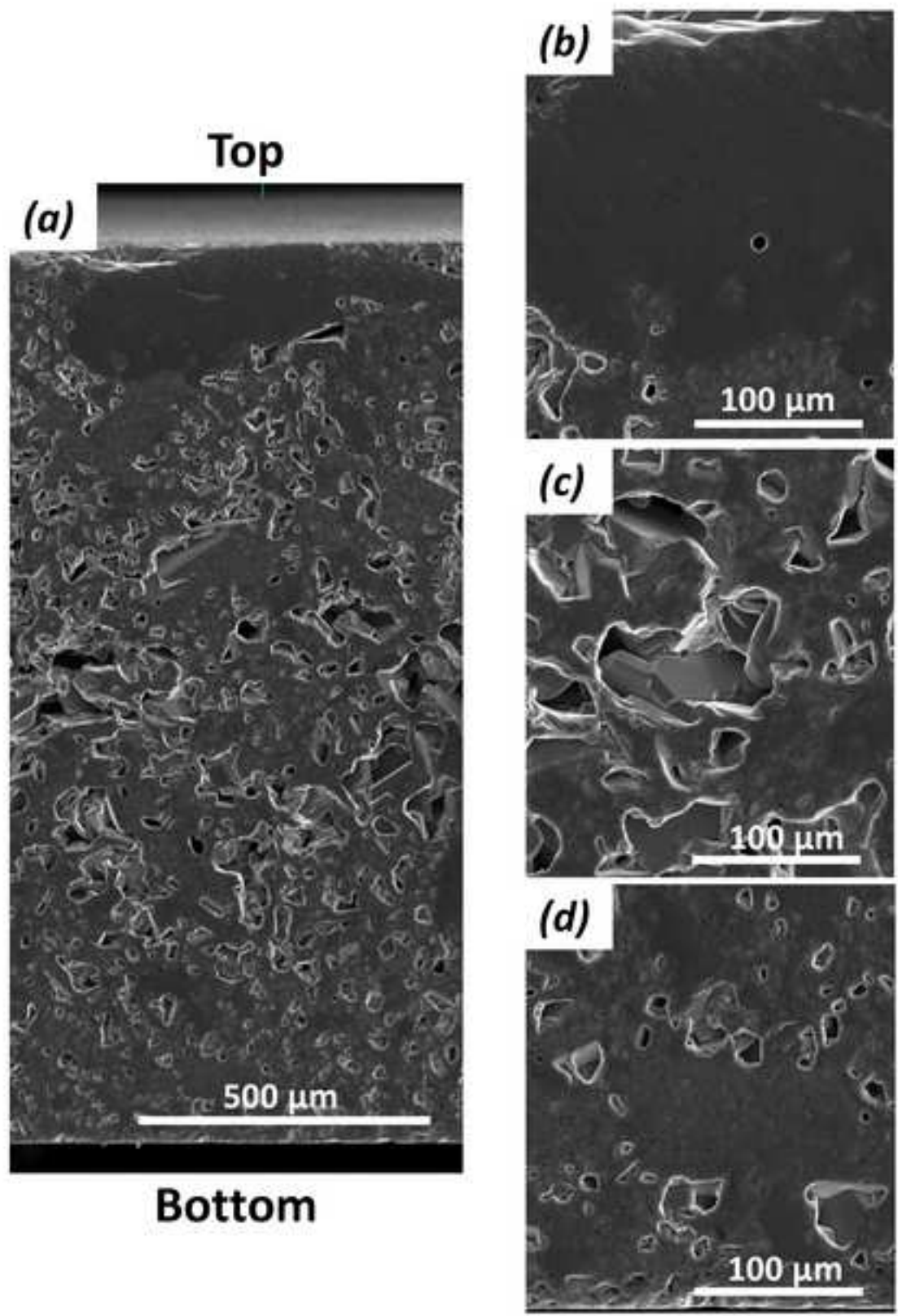


Figure 4  
[Click here to download high resolution image](#)

